

## Exploring Semiconductor Property in Charge Transfer Cocrystal of 1-Aminopyrene and TCNQ

Arkalekha Mandal,<sup>a\*</sup> Anwesha Choudhury,<sup>c</sup> Rahul Kumar,<sup>a</sup> Parameswar Krishnan Iyer,<sup>b,c\*</sup>  
Prasenjit Mal<sup>a\*</sup>

<sup>a</sup>School of Chemical Sciences, National Institute of Science Education and Research  
(NISER), HBNI, Bhubaneswar, PO Bimpur-Padanpur, Via Jatni, District Khurda, Odisha  
752050, India

<sup>b</sup>Centre of Nanotechnology, Indian Institute of Technology Guwahati, Guwahati, Assam,  
India, 781039.

<sup>c</sup>Department of Chemistry, Indian Institute of Technology Guwahati, Guwahati, Assam,  
India, 781039.

Corresponding Authors Email: [arkalekha@niser.ac.in](mailto:arkalekha@niser.ac.in) (AM); [pmal@niser.ac.in](mailto:pmal@niser.ac.in) (PM);  
[pki@iitg.ac.in](mailto:pki@iitg.ac.in) (PKI)

## Experimental Section

### *Materials and methods*

1-Aminopyrene, TCNQ and the solvents were used as received from commercial sources without further purification. The cocrystal was characterized using single crystal XRD, UV-Vis, FT-IR and EPR spectra as well as powder XRD, thermo-gravimetric (TGA) analyses of the powdered sample. The structure was solved by direct method using SHELXL-97.<sup>1</sup> Non hydrogen atoms were refined anisotropically by full matrix least-squares on  $F^2$ , using SHEXL while both C–H and N–H hydrogen atoms were added at the calculated positions ('constr' method of hydrogen atom addition) and were refined isotropically using a riding model. The parameters of intermolecular interactions were derived using PARST<sup>2</sup> programme and the crystal packing diagrams were obtained by Mercury 3.10.

### *Synthesis of cocrystal*

Equi-molar amounts of 1-aminopyrene (21 mg, 0.1 mmol) and TCNQ (20 mg, 0.1 mmol) were grinded with adding few drops of MeOH for 1 h to produce brownish red powder. Dark red crystals suitable of cocrystal **1** (CCDC: **1915543**) for X-ray study were grown by slow evaporation of toluene solution after four days. Melting point: 192 °C.

### *Computational methods*

The HOMO, LUMO energies and static dipole moment (SDM) were calculated on crystal geometry employing DFT calculations at M06-2X/6-311G(d,p) level of theory to take account of the dispersive nature of  $\pi\cdots\pi$  stacking interaction.<sup>3</sup> The electron and hole transfer integrals were calculated using frontier molecular orbital energies of AA/ DD dimers and ADA/ DAD trimers obtained from crystal geometries. Coulomb attenuated version of B3LYP (CAM-B3LYP) functional was used for accounting long range correction (LRC) in calculating transfer integrals.<sup>4</sup> Wavelength, oscillator strength and orbital contributions for

vertical electronic excitation were calculated by TD-DFT method using B3LYP/6-31G(d,p) level of theory on crystal coordinates. The interaction energy of dimeric D–A pairs were calculated at M06-2X/6-31G(d,p) level following basis set superposition error corrected (BSSE) method of Boys and Bernerdi.<sup>5</sup> Natural bond orbital (NBO) calculations were performed at M06-2X/6-31G(d,p) level of theory using NBO 3.1.<sup>6</sup> Intermolecular interactions in crystal packing were analysed quantitatively using analysis of the Hirshfeld surface ( $d_{norm}$  surface) with 2D fingerprint plots. Analysis of  $d_{norm}$  surface with 2D fingerprint plots provides concise description of all weak intermolecular interactions present in crystal packing. The red, white and blue regions on the  $d_{norm}$  surface of cocrystal respectively indicate short range contacts, contacts at van der Waals separation and the longer contacts.<sup>7</sup> Interaction energy of  $\pi$ -stacked D–A dimer was analysed with energy decomposition analysis<sup>8</sup> to determine the contribution of electrostatic, polarization, dispersion and repulsion energies ( $E_{total} = E_{electric} + E_{polarization} + E_{dispersion} + E_{repulsion}$ ). Electrostatic, polarization, dispersion and repulsion energy values were obtained with B3LYP-D2/6-31G(d,p) level of theory using Grimme's dispersion correction method. CrystalExplorer 17.5 version was used for all calculations.<sup>8</sup>

### **Device fabrication**

Keithley 4200SCS semiconductor parameter analyser was used for performing the Current-Voltage measurements. The measurements were done at room temperature and at the ambient atmosphere conditions. To check ability of the cocrystal to transport electrons, OFET was prepared with the cocrystal acting as the active layer. On cleaned glass substrates  $\approx 100$  nm thick aluminum gate was deposited by thermal evaporation which was followed by spin coating and annealing with PMMA solution at 100 °C for 30 min to form a layer of 1  $\mu$ m. On this layer cocrystal **1** in toluene solution (concentration of 30 mg/mL) were spin coated on separate substrates to form a layer of thickness  $\sim 100$  nm. Al source and drain contacts of

thickness ~80 nm were deposited on the active layer with channel length and width of 40  $\mu\text{m}$  and 1000  $\mu\text{m}$ , respectively. The field-effect mobility ( $\mu$ ) was calculated using the following

equation,  $\mu = \frac{L}{WC_i V_{DS}} \frac{\partial I_D}{\partial V_G}$  where, W and L respectively indicate width and length of channel,  $C_i$  (50 nF/cm<sup>2</sup>) is the capacitance per unit area of the gate dielectric layer, while the  $V_G$ ,  $V_{th}$  and  $V_{DS}$  are the gate, threshold and source-drain voltages, respectively. The  $\frac{\partial I_D}{\partial V_G}$  value is extracted from the slope of the transfer characteristic curve.

## Reference

1. G. M. Sheldrick, *Acta Cryst. C*, 2015, **71**, 3.
2. M. Nardelli, *J. Appl. Cryst.*, 1995, **28**, 659.
3. Y. Zhao and D. G. Truhlar, *Theor. Chem. Acc.*, 2007, **120**, 215.
4. A. Pedone, *J. Chem. Theory Comput.*, 2013, **9**, 4087.
5. S. F. Boys and F. Bernardi, *Mol. Phys.*, 1970, **19**, 553.
6. NBO Version 3.1, E. D. Glendening, A. E. Reed, J. E. Carpenter, F. Weinhold.
7. M. A. Spackman and J.J. McKinnon, *CrystEngComm*, 2002, **4**, 378.
8. J. J. McKinnon and D. Jayatilaka, M.A. Spackman, *Chem Commun.*, 2007, 3814.

**Table S1.** Crystallographic and refinement parameters for cocrystal **1**

Parameters	Cocrystal <b>1</b>
chem formula	C <sub>28</sub> H <sub>15</sub> N <sub>5</sub>
formula wt	421.45
temp (K)	296
Radiation wavelength	1.54184 Å
CCDC Number	1915543
crystal system	Triclinic
space group	<i>P</i> -1
<i>a</i> (Å)	6.7858(2)
<i>b</i> (Å)	8.7123(2)
<i>c</i> (Å)	18.1329(4)
$\alpha$ (°)	99.099(2)
$\beta$ (°)	91.152(2)
$\gamma$ (°)	97.907(2)
<i>V</i> (Å <sup>3</sup> )	1047.50(5)
<i>Z</i>	2
$\rho_{\text{calc}}$ (g cm <sup>-3</sup> )	1.336
no. of unique rflns	4215
no. of rflns ( $I \geq 2\sigma(I)$ )	3240
R <sub>1</sub> <sup>a</sup> , R <sub>1</sub> <sup>b</sup> (all data, $I \geq 2\sigma(I)$ )	0.1352, 0.1199
wR <sub>2</sub> <sup>a</sup> , wR <sub>2</sub> <sup>b</sup> (all data, $I \geq 2\sigma(I)$ )	0.2819, 0.2771
goodness of fit ( $F^2$ )	1.021
largest peak/hole (e Å <sup>-3</sup> )	0.375/ -0.270

**Table S2.** Parameters of hydrogen bonding interactions in cocrystal **1**.

Interaction	D...A (Å)	H...A (Å)	D-H...A (°)	Symmetry
N1-H1B...N2	3.429(9)	2.58	168	-x+1, -y, -z
N1-H1A...N3	3.472(9)	2.64	163	-x+1, -y+1, -z
C18-H18...N4	3.604(8)	2.80	146	x, y+1, z
C21-H21...N3	3.589(7)	2.77	148	x, y-1, z
C13-H13...N2	3.592(8)	2.66	178	-x+1, -y, -z
C6-H6...N5	3.477(9)	2.83	128	-x+1, -y+1, -z+1
C21-H21...N4	3.580(9)	3.00	122	x, y, z

**Table S3.** Calculation of super-exchange transfer integrals (meV) from ADA/ DAD triads and energy difference between bridge orbitals in super-exchange pathway (meV) in reported 1:1 pyrene:TCNQ charge transfer cocrystal, crystal coordinates used for calculation

Parameters	1:1 Pyrene: TCNQ
$t_e^{\text{super}}$ (meV)	29.4
$t_h^{\text{super}}$ (meV)	11.3
D-A-D or A-D-A trimer	
$t$ [(HOMO-1)/LUMO] (meV)	129.3
$t$ [HOMO/LUMO] (meV)	205.6
$\Delta E$ [(HOMO-1)/LUMO] (meV)	1439
$\Delta E$ [HOMO/LUMO] (meV)	569

**Table S4.** TD-DFT calculation for cocrystal **1** at M06-2/6-311G(d,p) level of theory

Calculated wavelength $\lambda$ (nm)	Oscillator strength $f$	Transition electric moment (D)	Transition energy (eV)	Orbital contributions
1162	0.0088	0.210	1.07	HOMO→LUMO, 100%
476	0.0566	0.173	2.62	HOMO-1→LUMO, 100%
390	0.3720	1.965	3.18	HOMO-2→LUMO, 75% HOMO→LUMO+1, 75%

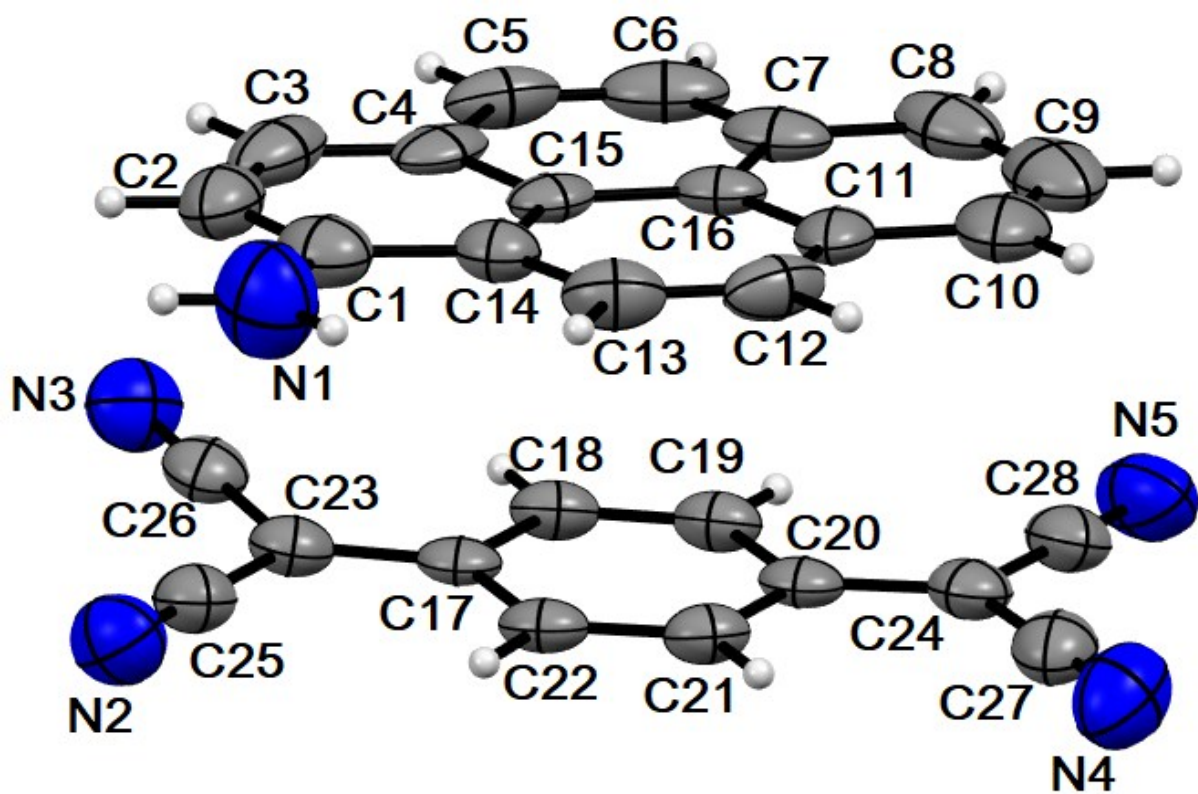


**Fig. S1** ORTEP diagram (50% thermal probability of ellipsoids) of cocystal 1.

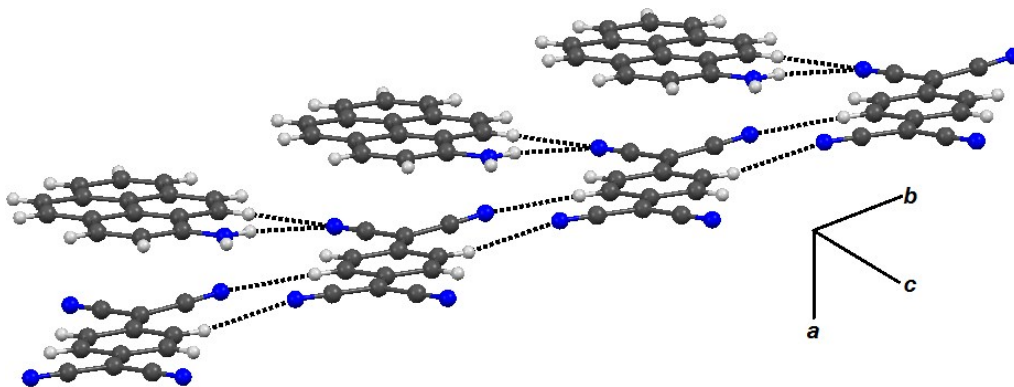


**Fig. S2** Multiple C–H···N hydrogen bonds forming a two dimensional array in crystal packing of cocystal 1.

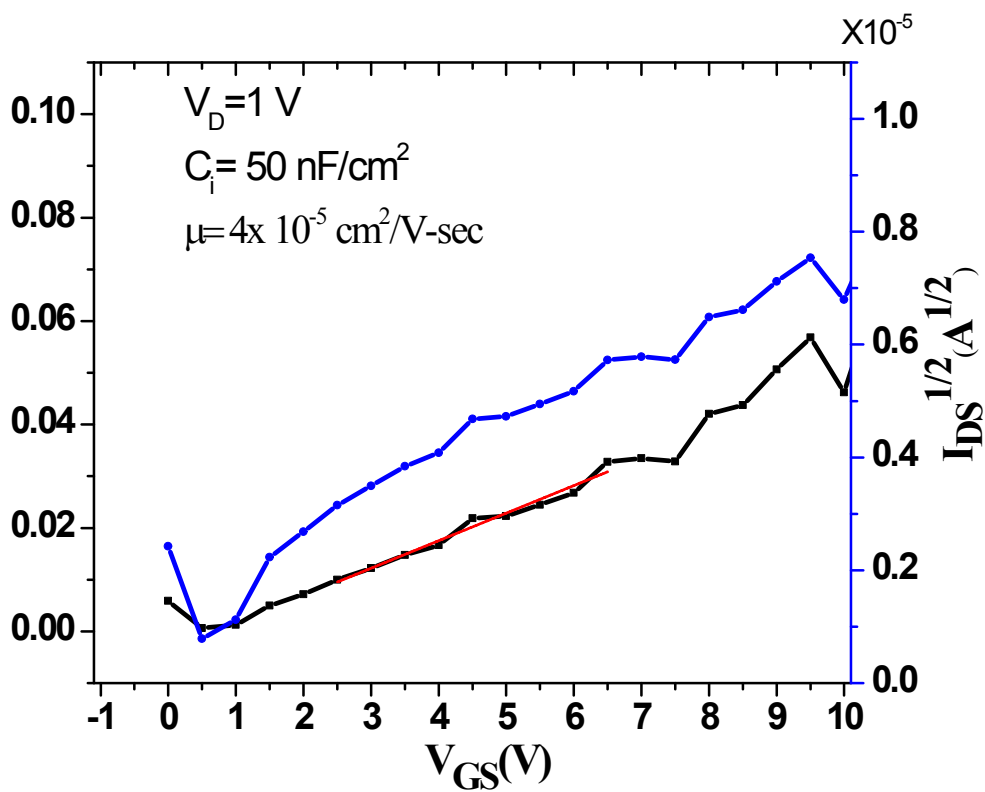
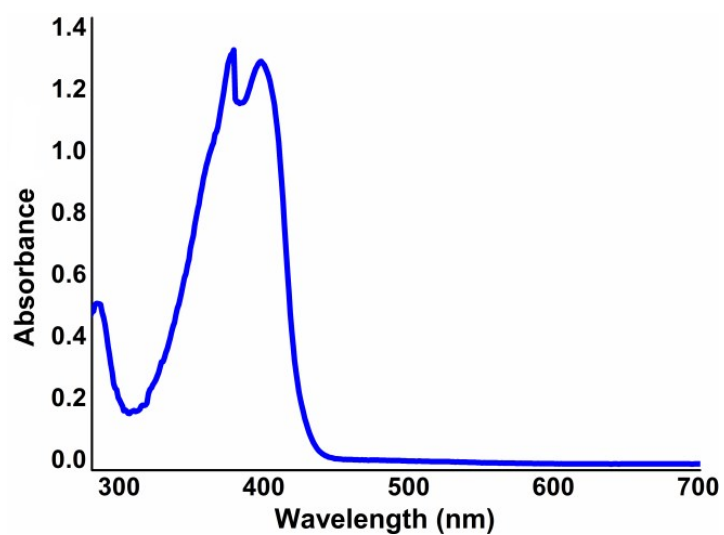
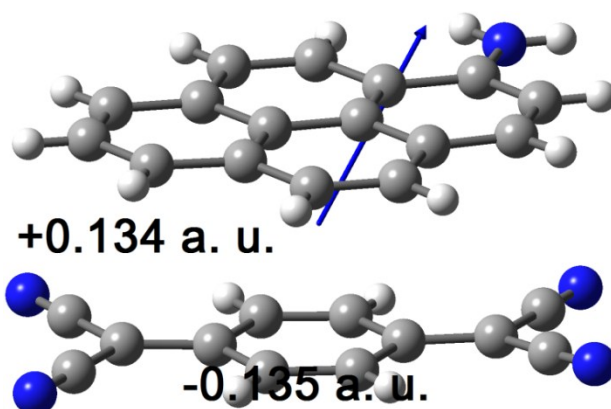


Fig S3. Electron transfer characteristic of cocystal 1.





**Fig. S4** UV-Vis spectrum of cocystal **1** in MeCN solution ( $c = 10^{-5}$  M) shows no occurrence of charge transfer.



**Fig. S5** Mulliken charge distribution in cocystal **1**.

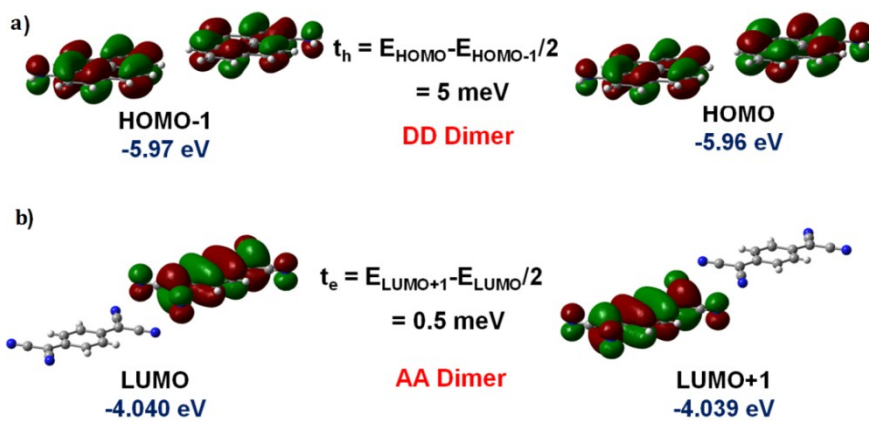


**Fig. S6** Direct hole ( $t_h^{\text{super}}$ ) and electron transfer ( $t_e^{\text{super}}$ ) integrals in cocrystal **1**, calculated at CAM-B3LYP/6-311G(d,p) level of theory.

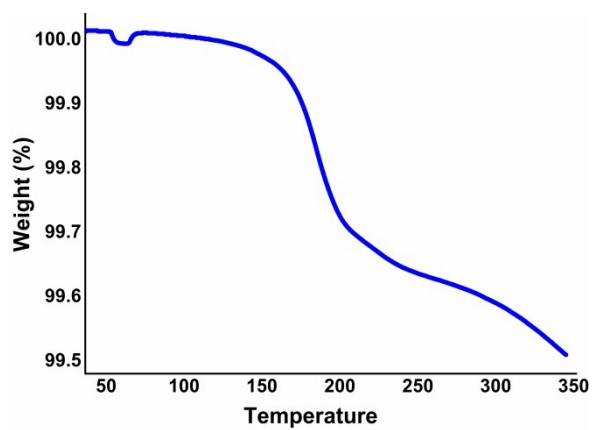


**Fig. S7** Thermo-gravimetric analysis of cocrystal **1** shows decay at 200°C.

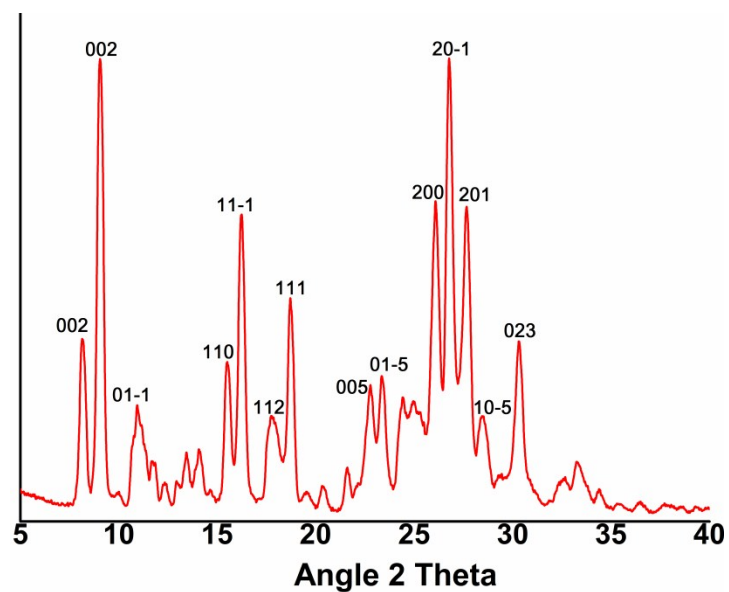


**Fig. S8** Powder XRD of cocrystal 1 shows high purity of the bulk phase.

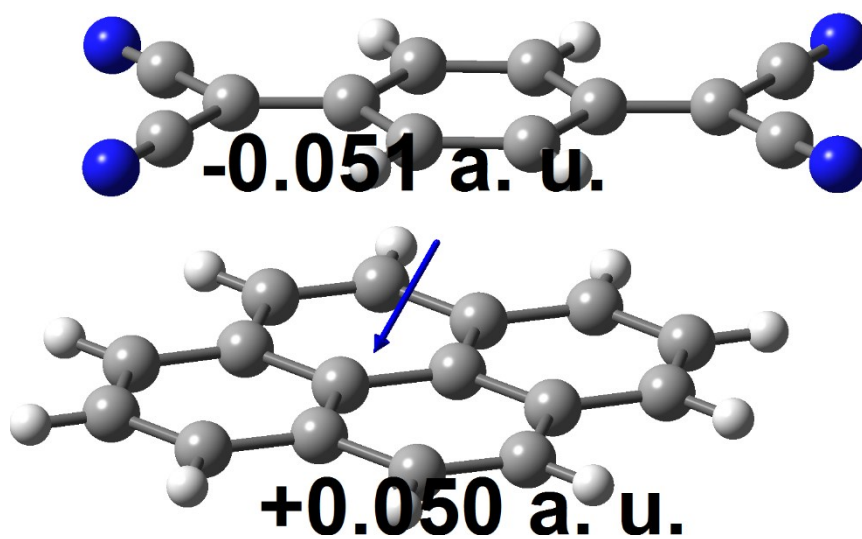


**Fig. S9** Mulliken charge distribution in reported 1:1 pyrene:TCNQ cocrystal.

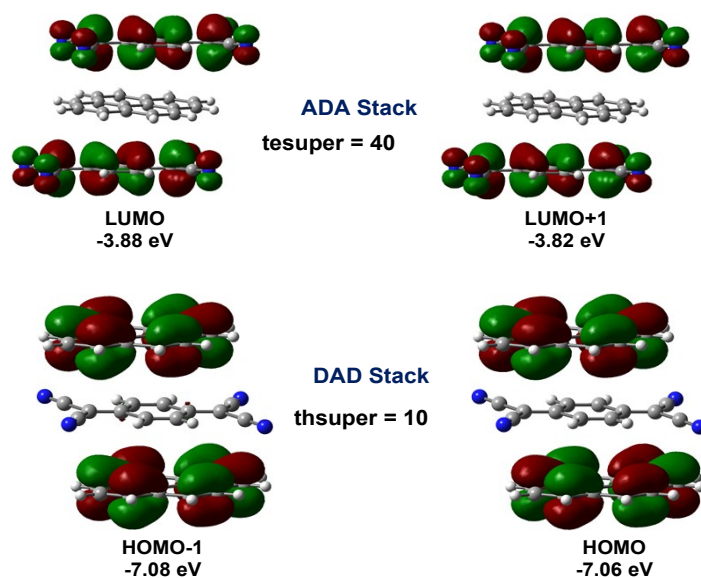


**Fig. S10** Super-exchange hole ( $t_h^{\text{super}}$ ) and electron transfer ( $t_e^{\text{super}}$ ) integrals in reported 1:1 pyrene:TCNQ cocrystal, calculated at CAM-B3LYP/6-311G(d,p) level of theory.

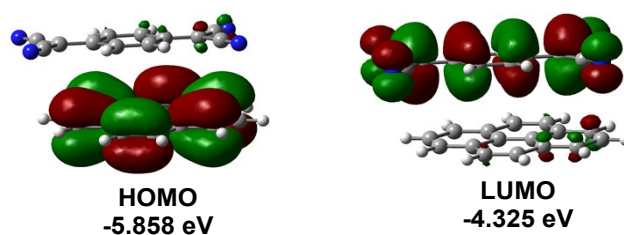


**Fig. S11** The HOMO and LUMO distribution in reported 1:1 pyrene:TCNQ cocrystal.

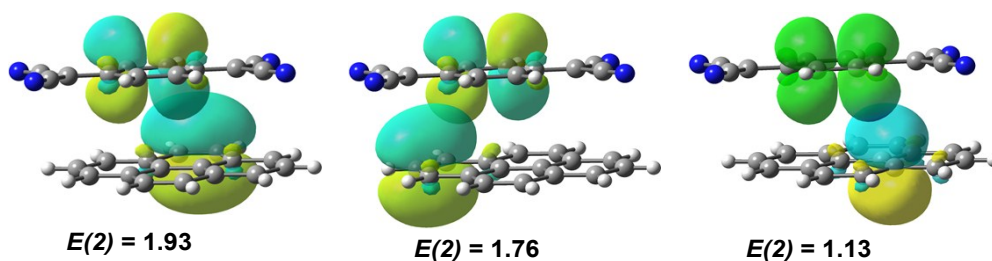


**Fig. S12** Natural bond orbital (NBO) analyses in reported 1:1 pyrene:TCNQ cocrystal.

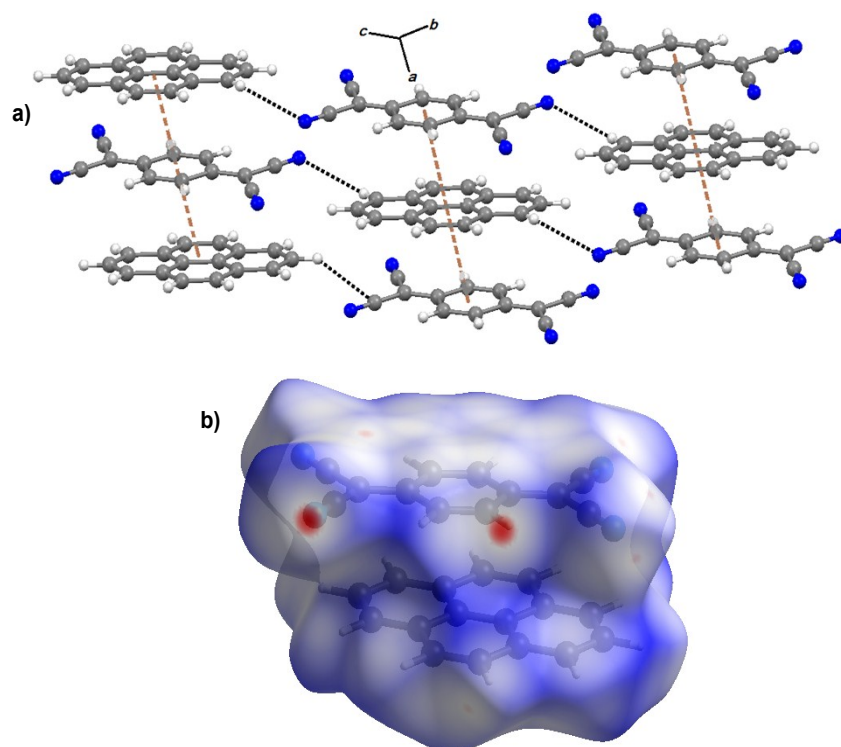


**Fig. S13** (a) Crystal packing of reported 1:1 pyrene:TCNQ cocrystal; (b) The  $d_{norm}$  surface of pyrene:TCNQ cocrystal.